Adatom Transport on Strained Cu(001): Surface Crowdions

Wei Xiao, P. Alex Greaney, and D. C. Chrzan

Department of Materials Science and Engineering, University of California, Berkeley, California, 94720

(Received 3 November 2002; published 14 April 2003)

Surface strain is often suggested as a means to control the self-assembled growth of nanostructures. Strain affects both the kinetics of nucleation and the free energies of formation of the desired nanostructure. It is demonstrated here that diffusion on some strained surfaces may be mediated by newly identified adatom transport mechanism: the formation and motion of a surface crowdion.

DOI: 10.1103/PhysRevLett.90.156102 PACS numbers: 68.43.Jk, 61.72.Cc, 61.72.Ji

The technological promise of highly ordered nanostructures is manifest. However, this promise can be realized only if the nanostructures can be produced reliably and economically. To address this need, the nanostructure processing community has turned to so-called self-assembly methods in which the ordered nanostructured device arises spontaneously as a result of the growth process.

It has been proposed that strain might be used to self-assemble two-dimensional ordered arrays of nanocrystals using traditional thin film growth techniques, for example, molecular beam epitaxy [1–3]. The strain influences the growth process in two important ways: the strain affects both the kinetics of nucleation and the free energy of formation of the growing nanostructure.

Consider the self-assembled formation of an ordered array of nanocrystals using traditional molecular beam epitaxy methods. A key component of the kinetics of nanocrystal nucleation is the diffusion of adatoms on the surface of the strained substrate. Adatom diffusion is known to be influenced by surface strain, and the details of how strain impacts the diffusion process are beginning to be understood. Theory has played a major role in the study of the kinetics of nucleation and growth in thin films (see, for example, [4–6]), and theory has been used to address directly the energy barriers to adatom diffusion [7] including the dependence on strain [8–10].

This Letter focuses on an aspect of the strain dependence of diffusion on (001) surfaces of face-centered-cubic (fcc) metals that had not yet been considered. Cu adatoms on Cu(001) are studied as a prototypical system, employing strain states that are potentially accessible to direct study via traditional thin film growth techniques. Though the details of the calculations presented here certainly depend on the potential employed, one expects similar behavior in other fcc materials.

There is much known about diffusion on the {001} surfaces of fcc materials. Two competing mechanisms have been identified in the literature: hopping, in which an adatom "hops" over a neighboring bridge site to one of its nearest neighbor sites (i.e., a site along a ⟨110⟩ direction), and a mechanism referred to here as "kick-out" in which the adatom displaces a substrate atom in one of the ⟨100⟩ directions in the plane of the surface (see Fig. 1) [7,11,12]. The energy barriers to these two different processes can be computed using the nudged elastic band technique [13]. In this technique, one identifies the minimum energy path in configuration space between an initial and final configuration. The highest energy along this path is then the energy barrier for the process, and the associated configuration of atoms is referred to as the "saddle point" configuration.

Hopping and kickout have significantly different paths in configuration space, and one expects that they might be influenced by surface strains in markedly different ways. Atomic scale total energy calculations can be used to explore this strain dependence. The calculations presented here employ the embedded atom method (EAM) interatomic potentials for Cu developed by Foiles *et al.* [14]. Force calculations are carried out using the code XMD [15] coupled to our own implementation of the nudged elastic band method. The x and y directions are chosen to be the [110] and [$\bar{1}$10] directions, respectively. Uniform strain states in the range $-0.04 \leq \varepsilon_{xx}, \varepsilon_{yy} \leq 0.04$ are considered [16]. The calculations employ a six layer slab of atoms composed of 1201 atoms (1200 substrate atoms,

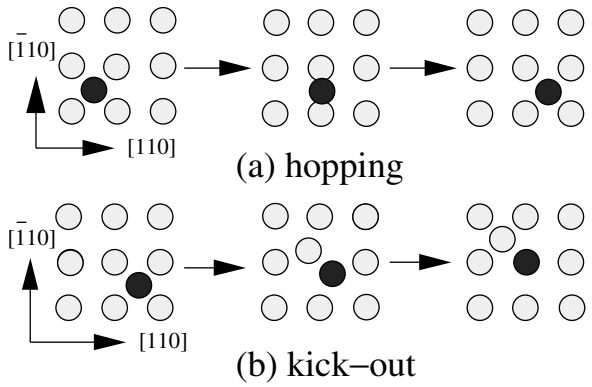

FIG. 1. Schematic of two of the adatom transport mechanisms studied in this paper. The [001] direction points out of the page. Gray atoms are initially substrate; black atoms are initially adatoms. Panel (a) depicts the simple hopping mechanism. Panel (b) depicts the mechanism referred to here as kick-out. The central configuration is the saddle point configuration.

and one adatom, see Fig. 2). Periodic boundary conditions are applied in plane (the x and y directions), and the surfaces are free to relax in the (001) direction. Calculations are converged completely with respect to cell size. Typically, the path in configuration space is modeled by 15 discrete states or images. Forces on the images are converged to better than 0.01 eV/Å, and the quoted energy barriers are computed to an accuracy of better than 0.05 eV. For the unstrained surface, the computed energy barrier for hopping is 0.51 eV, in good agreement with the values of 0.5 and 0.48 eV computed with the EAM method by Boisvert and Lewis [17] and Mehl *et al.* [18], respectively. The computed kickout energy barrier is 0.70 eV which is in good agreement with Boisvert's 0.73 eV barrier for kickout [17]. The energy barrier for surface diffusion of copper has been measured experimentally by Durr *et al.* to be 0.36 eV [19].

Consider first the application of a tetragonal strain. (Here, the phrase tetragonal strain refers to the case for which $\varepsilon_{xx} = \varepsilon_{yy}$. Nontetragonal strains have $\varepsilon_{xx} \neq \varepsilon_{yy}$. The strain ε_{zz} is determined by the relaxation of the unit cell.) The energy barriers for both hopping and kickout are plotted as a function of this strain in Fig. 3. There are four features of this plot that warrant comment. First, the energy barrier for hopping increases with increasing tensile strain, a trend also apparent in the work presented in Refs. [8,10]. Second, the energy barrier for the kickout process decreases with increasing tensile strain. Third, the changes in the kickout energy barrier with strain are substantial, approximately 0.75 eV over the range shown. Fourth, there is a strain at which the energy barriers associated with the two processes cross.

Consider the causes and implications of these four observations. The strain dependence of the energy barriers results from the strain dependence of both the adatom adsorption energy and the saddle point energy. For simple hopping, a tensile strain increases the energy barrier to hopping. Analysis of the surface relaxations associated with this mechanism suggests the following origins for this dependence [10]. As the substrate undergoes tensile strain an adatom is better able to relax into the substrate surface, increasing its local electron density, thereby increasing its adsorption energy. At the saddle point the substrate atoms beneath the hopping atom separate, facilitating the passage of the adatom. Increasing tensile strain allows for more movement of the substrate atoms and so better relaxation. However, the hopping atom is in its least coordinated state at the saddle point. Consequently, the strain has a less strong influence on the saddle point energy than on the initial state energy and the barrier for hopping rises with tensile strain.

The saddle point configuration for the kickout mechanism (Fig. 1), requires that the adatom "burrow" into the surface. It is reasonable to expect that this burrowing will cost less energy for a surface under significant tensile strain than for a compressed surface, and this too, is consistent with the observed behavior. This effect is significant. A change in energy barrier of 0.75 eV would be

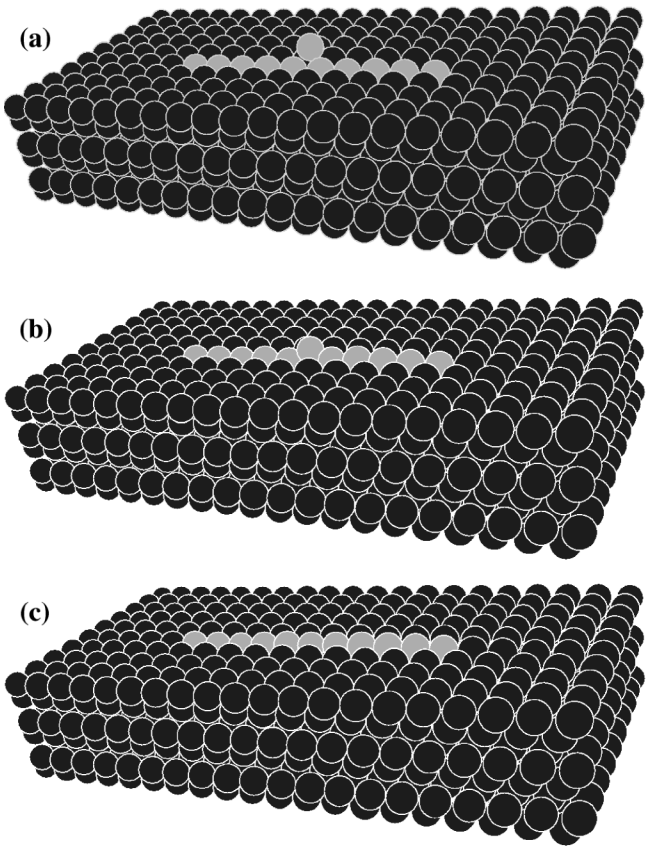

FIG. 2. The formation and structure of a surface crowdion in the unit cell used in the computations. Panel (a) is the initial configuration. Panel (b) is the saddle point configuration. Panel (c) shows the crowdion fully formed. The crowdion extends along the [110] direction (tensile direction) for roughly 10 nearest neighbor spacings. There is a compressive strain along [$\bar{1}$10].

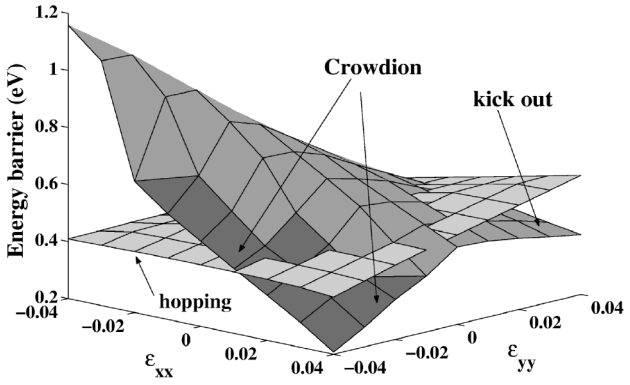

FIG. 3. The energy barriers associated with the adatom transport mechanisms identified in Figs. 1 and 2. The energy barriers plotted as a function of strain state. One surface presents the barrier for hopping, the other for kick-out and crowdion formation. Since the crowdion is a metastable state that forms during kick-out, they share a single energy surface.

clearly observable. It is important to note that the kickout mechanism does not transport a *single* atom across the surface of the substrate. Instead, the adatom initiating the process becomes a substrate atom, and the neighboring atom becomes the adatom. In heterogeneous systems such as the growth of metal multilayers, kickout may lead to intermixing of the species, resulting in a rougher interface between the two materials. Under these circumstances, it is apparent that strain may be used to inhibit the intermixing.

The final observation, that the energy barriers cross at a tetragonal strain of $\varepsilon_{xx} = \varepsilon_{yy} \approx 0.016$, suggests that at reasonable temperatures, the dominant adatom diffusion mechanism is strain dependent. Under tensile tetragonal strains, kickout is favored, while under compressive strains, hopping dominates. The change in diffusion mechanism affects the rate of nucleation and growth processes on the surface. For example, changes in the adatom diffusion constant impact the density of nucleated islands. However, tetragonal strains do not break the fourfold symmetry of the surface, and will not alter significantly the shapes of nucleated islands. Application of nontetragonal strains, i.e., $\varepsilon_{xx} \neq \varepsilon_{yy}$, may have a more pronounced effect on the nucleation and growth process, as well as the shapes of the nucleated islands, and strain states of this type are now considered.

Figure 3 also depicts the energy barriers for the kickout and hopping mechanisms as a function of nontetragonal strain. This plot reveals interesting features of the kickout mechanism energy barrier. The different shades of gray on the energy surface for kickout indicate a change in adatom transport mechanisms. In regions of maximum shear strain, e.g., those regions for which $\varepsilon_{xx} \approx -\varepsilon_{yy} \approx 0.03$, the reaction path takes the system through a metastable structure, a surface crowdion. The recorded energy barrier is then the barrier to formation of this surface crowdion.

The structure of the surface crowdion is shown in Fig. 2(c). The saddle point configuration for the crowdion [Fig. 2(b)] is similar to that observed for the kickout mechanism, but as the reaction configuration progresses, the structure transforms to a metastable (sometimes stable) state in which the adatom is embedded into the surface, and a needlelike defect aligned along a $\langle 110 \rangle$ direction forms. This defect is the surface crowdion. The crowdion extends over roughly ten nearest neighbor distances, and appears only for stress states that are compressive along the axis normal to the needle direction, and tensile along the direction of the needle. The crowdion, once formed, can move along the row of atoms by relatively small changes in the positions of the atoms: the computed energy barrier for moving between symmetrically equivalent sites along the needle direction is of the order of 0.001 eV. Further, the defect may be "born" with some kinetic energy gained from descending the energy surface from the saddle point to the metastable crowdion configuration. The implication is that once formed, the crowdion may lead to apparent transport of the adatom over significant distances, ballistic transport limited only by the scattering of the crowdion with other crowdions, adatoms, or phonons. As in the case of kickout, the initial adatom becomes a substrate atom, and a substrate atom becomes a new adatom. In contrast to kickout, however, the new adatom is not necessarily a nearest neighbor of the original diffusing adatom.

The factors stabilizing the crowdion are readily apparent. Figure 1(b) indicates the saddle point configuration of the kickout mechanism for the unstrained surface. On the unstrained (and tetragonally strained) surface, the atoms are aligned perfectly along a $\langle 100 \rangle$ direction at the saddle point. When the fourfold symmetry of the substrate is broken by the introduction of a nontetragonal biaxial strain state, the saddle point configuration begins to rotate so that the axis of the "bond" between the two central atoms of Fig. 1(b) skews in the $\langle 110 \rangle$ direction corresponding with the tensile direction of the strain. The tensile load enhances the tendency for a surface adatom to burrow into the surface and the compressive component of the stress helps to rotate the crowdion into the state aligned along a $\langle 110 \rangle$ direction (Fig. 2). The simple physics underlying crowdion formation suggest that crowdions may be present on the strained {001} surfaces of other fcc metals.

Crowdions have been studied in bulk copper [20] since the late 1950's. However, to the knowledge of the current authors, this is the first time that crowdions have been suggested as a mechanism for surface adatom transport. Their presence on surfaces is sure to impact dramatically the nucleation and growth processes on strained substrates.

The proposed crowdion mediated transport is extremely anisotropic. Motion along the crowdion formation direction will be ballistic, while motion along other directions will be governed by simple hopping. Knowledge of the effective mass of the crowdion, estimates of the attempt frequencies for crowdion formation and simple adatom hopping, and understanding of the crowdion phonon interaction, should allow one to define an effective anisotropic diffusion coefficient as a function of strain.

One can estimate the kinetic energy of the traveling crowdion by relating the velocities of individual atoms in the crowdion to the crowdion velocity. The effective mass of the crowdion is then obtained from the classical definition of the kinetic energy. The estimated effective mass is approximately 0.07 the mass of a bare Cu atom. Assuming that the crowdion is a classical, one-dimensional particle born with room temperature kinetic energy, one deduces that the crowdion velocity is approximately 750 m s^{-1}. While this large computed velocity casts doubt on the accuracy of the simple approximation, it demonstrates clearly that crowdion mediated transport should be substantially more efficient than simple adatom

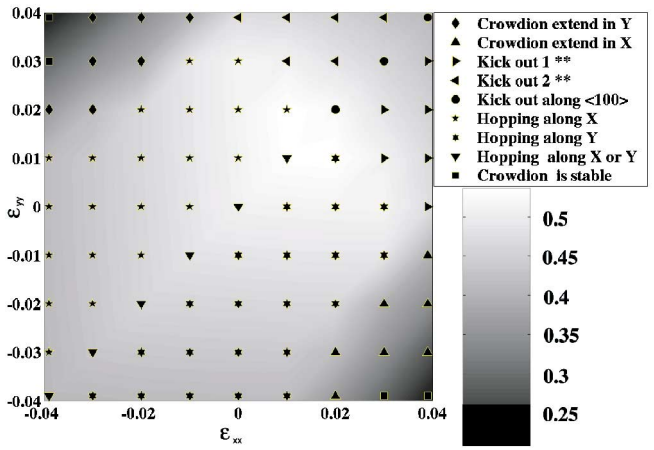

FIG. 4 (color online). Adatom transport mechanism map. The symbols indicate the mechanism with the lowest energy barrier at the given strain. In the case of kick-out and hopping, this is the energy barrier to adatom transport. In the case of the crowdion, the reported barrier is the energy barrier to crowdion formation. Under extreme shear strains (for example $\varepsilon_{xx} = -\varepsilon_{yy} = 0.4$, the initial adatom surface configuration is unstable with respect to the formation of the crowdion. For these strain states, the current analysis is not applicable. ** The saddle point configuration of the kick out mechanism is altered by the imposed strain. For nontetragonal strains, the ''bond'' between the two central atoms of Fig. 1(b) does not lie in a $\langle 100 \rangle$ direction. During kick-out 1, the ''bond'' rotates toward the [110] direction. In kick-out 2, the bond rotates towards the $[\bar{1}10]$ direction.

hopping or kickout, and will yield extremely anisotropic diffusion.

This anisotropic diffusion, then, will be readily apparent in the shapes and distributions of nucleated islands during submonolayer homoepitaxy [21]. Further, because this transport mechanism is expected to be so highly anisotropic, it should be discernible from the small anisotropy expected from the effect of the imposed strain state on adatom motion via the simple hopping and kickout mechanisms.

To further clarify the strain dependence of the dominant adatom transport mechanism we have constructed an adatom transport mechanism map (Fig. 4). This map identifies the adatom transport mechanism with the lowest energy barrier for each of the studied strain states. Hence this map indicates which transport mechanism will be most prevalent at very low temperatures. Of course, at all temperatures, all of the identified mechanisms will be active, with their relative importance dictated by their absolute relative rates. Hence even though the energy barrier to formation of a surface crowdion may exceed that for simple adatom hopping, the formation of the crowdion may be an important contribution to adatom transport. The mechanism map, when coupled with the energy surface plot in Fig. 3 indicate the strain states at which the crowdion is likely to be active.

The implications for our understanding of nucleation and growth, and, in particular, the control of nucleation and growth through strain are profound. The present study indicates that strain can have dramatic and unexpected consequences for adatom transport during nucleation and growth, including the introduction of entirely new mechanisms for adatom transport.

The authors acknowledge stimulating discussions with K. J. Cho, B. M. Clemens, J.W. Morris, Jr., W. D. Nix, J. Sethna, and M. P. Surh. The authors acknowledge the financial support of the National Science Foundation under Grant No. EEC-0085569 and computational support from the Metals Program, Materials Sciences Division, Lawrence Berkeley National Laboratories.

[1] J. Tersoff, C. Teichert, and M. G. Lagally, Phys. Rev. Lett. **76**, 1675 (1996).
[2] A. E. Romanov, P. M. Petroff, and J. S. Speck, Appl. Phys. Lett. **74**, 2280 (1999).
[3] K. Bromann, M. Giovannini, H. Brune, and K. Kern, Eur. Phys. J. D **9**, 25 (1999).
[4] M. C. Bartelt and J.W. Evans, Phys. Rev. B **46**, 12 675 (1992).
[5] G. S. Bales and D. C. Chrzan, Phys. Rev. B **50**, 6057 (1994).
[6] J. G. Amar and F. Family, Phys. Rev. Lett. **74**, 2066 (1995).
[7] P. J. Feibelman, Phys. Rev. Lett. **65**, 729 (1990).
[8] M. Schroeder and D. E.Wolf, Surf. Sci. **375**, 129 (1997).
[9] C. Roland and G. H. Gilmer, Phys. Rev. B **46**, 13428 (1992).
[10] C. Ratsch, A. P. Seitsonen, and M. Scheffler, Phys. Rev. B **55**, 6750 (1997).
[11] G. L. Kellogg and P. J. Feibelman, Phys. Rev. Lett. **64**, 3143 (1990).
[12] G. L. Kellogg, Appl. Surf. Sci. **87–88**, 353 (1995).
[13] H. Jonsson, G. Mills, and K.W. Jacobsen, in *Classical and Quantum Dynamics in Condensed Phase Simulations*, edited by B. J. Berne, G. Ciccotti, and D. F. Coker (World Scientific, Singapore, 1998), p. 385.
[14] S. M. Foiles, M. I. Baskes, and M. S. Daw, Phys. Rev. B **33**, 7983 (1986).
[15] Jon Rifkin, University of Connecticut, http://www.ims.uconn.edu/centers/simul
[16] Local strains in this range should be accessible on the surfaces of misfit dislocated thin films. P. A. Greaney (unpublished).
[17] G. Boisvert and L. J. Lewis, Phys. Rev. B **56**, 7643 (1997).
[18] H. Mehl, O. Biham, L. Furman, and M. Karimi, Phys. Rev. B **60**, 2106 (1999).
[19] H. Durr, J. F. Wendelken, and J. K. Zuo, Surf. Sci. **328**, L527 (1995).
[20] L. Tewordt, Phys. Rev. **109**, 61 (1958).
[21] S. Günther, E. Kopatzki, M. C. Bartelt, J.W. Evans, and R. Behm, Phys. Rev. Lett. **73**, 553 (1994).